

**Effective encapsulation of laccase in an aluminium silicate  
nanotube hydrogel**

Journal:	<i>New Journal of Chemistry</i>
Manuscript ID:	Draft
Article Type:	Paper
Date Submitted by the Author:	n/a
Complete List of Authors:	Kato, Katsuya; National Institute of Advanced Industrial Science and Technology, Advanced Manufacturing Research Institute Inukai, Keiichi; AIST, Fujikura, Kie; Nagoya Institute of Technology, Kasuga, Toshihiro; Nagoya Institute of Technology,

## ARTICLE

## Effective encapsulation of laccase in an aluminium silicate nanotube hydrogel

Cite this: DOI: 10.1039/x0xx00000x

Katsuya Kato,<sup>\*a</sup> Keiichi Iukai,<sup>a</sup> Kie Fujikura<sup>b</sup> and Toshihiro Kasuga<sup>b</sup>

Received 00th January 2012,  
Accepted 00th January 2012

DOI: 10.1039/x0xx00000x

www.rsc.org/

Aluminium silicate nanotubes (ASNT), with a length to width ratio of four, were synthesized from aluminium chloride and sodium silicate, and the ASNT hydrogel was easily prepared by adjusting to pH 7. The hydrogel nanotube concentration was 1.5 wt%. Laccase, a type of oxidase, was encapsulated during ASNT hydrogel formation. This encapsulation method will have fewer negative effects on the relatively unstable enzyme because of the milder conditions used, which are different from sol–gel silica formation by acidic catalysis using strong acids such as hydrochloric acid. The obtained hydrogels were fully characterized by various methods such as field-emission scanning electron microscopy and Fourier transform infrared spectroscopy. The ASNT-hydrogel encapsulated enzyme worked well; notably, laccase-ASNT hydrogels prepared from the shortest nanotubes exhibited higher activity than the free laccase in solution because of an improvement in substrate affinity of the encapsulated enzyme. Tryptophan fluorescence spectroscopy indicated that the highly ordered structure of laccase was not altered once bound to nanotubes within the hydrogel. Notably, after nine repeated reactions, laccase encapsulated in ASNT hydrogel retained its activity. The cycle performance of the encapsulated enzyme indicates no enzyme was released from the ASNT hydrogel. In addition, the laccase-ASNT hydrogel was easily used to prepare transparent thin films on glass cover slips, while still maintaining enzyme activity. Another oxidase, myoglobin, was also encapsulated in the same type of ASNT hydrogel. Although free myoglobin in solution demonstrated oxidation activity, the bound protein's activity was remarkably decreased due to changes in its tertiary structure when inside the ASNT hydrogel.

### Introduction

Encapsulation technologies have attracted considerable attention because of an increased interest in fields such as biotechnology, medicine, pharmaceuticals, catalysis, ecology and nutrition.<sup>1–3</sup> Encapsulation can concentrate and shield biomolecules to protect them in a defined volume and to create a single compartment that represents a microenvironment separated from the outer environment. Biomolecules have industrial applications based on various chemical and physical methods such as solvent evaporation, coacervation, interfacial polymerization and matrix (organic or inorganic) entrapment.<sup>4–6</sup> As an effective encapsulation technique, there are several strategies for encapsulating biomolecules in sol–gel silica materials.<sup>7–10</sup> However, most of the strategies are based on the usual process, in which alkoxysilanes are mixed with an alcohol and polymerized in the presence of acidic or basic conditions. Although this method has been used successfully for many years, it involves heating the particles to temperatures well

above ambient temperature and the use of highly basic pH; both conditions are destructive for proteins and other biomolecules.

The typical aluminium silicate nanotube material, imogolite, is a naturally occurring single-walled nanotubular aluminium silicate with an empirical formula of  $(\text{OH})_3\text{-Al}_2\text{O}_3\text{SiOH}$ .<sup>11–13</sup> Imogolite has an inner diameter of around 1.0 nm, an external diameter of around 2.5 nm and a length ranging from hundreds of nanometres to the micrometre scale. The inner surface of the nanotubes comprises Si–OH groups, while the outer surface is covered in Al–OH groups. These hydroxyl groups make the nanotubes hydrophilic, and the positive charges on the outer surface under acidic condition allow the nanotubes to be highly dispersed in water because of electrostatic repulsion. Recently, the use of imogolite as filler for organic/inorganic composites, electron emitter, support for nano-sized noble metals and shape-selective catalysts has been attempted.<sup>14–17</sup> In addition, the dispersibility of imogolite in water changes dramatically depending on pH, i.e. imogolite disperses as monofilaments or thin bundles in aqueous acidic

solutions (pH 4); in contrast, imogolite assembles into thick bundles or networks when pH is increased, and the resulting hydrogels form around pH 7.

Hydrogels are hydrophilic, three-dimensional networks that are able to encapsulate large amounts of water or biological fluids; thus they resemble, to a large extent, a biological tissue. Hydrogels are insoluble due to the presence of chemical (tie-points, junctions) and/or physical crosslinks such as entanglements, crystallites and phase separation.<sup>18–20</sup> Thus, aluminium silicate nanotube (ASNT) hydrogels have been adopted for encapsulation of biomolecules. Takahara *et al.* have reported on the encapsulation of the hydrolytic enzyme, pepsin, and deoxyribonucleic acid in ASNT hydrogel.<sup>21–23</sup> Within the ASNT hydrogel, pepsin was evenly dispersed throughout. Compared to the free enzyme in solution, pepsin immobilized within the hydrogel can be easily recovered from the reaction system, and can be used repeatedly. To the best of our knowledge, only the two above-mentioned reports were published about the encapsulation of biomolecules within the ASNT hydrogel. As different bio-applications of ASNT, we recently reported on the ASNT modification of the surface of inorganic–organic hybrid materials, and on cell culture tests of these materials. The new materials demonstrated that the initial adhesion of murine osteoblast-like cells on the surface of the fibres was enhanced by surface modification.<sup>24,25</sup>

Biocatalysts such as enzymes have been immobilized on supports by several methods including cross linking, covalent attachment, physical entrapment and physical adsorption. The solid supports used are always polymer resins, natural polymeric derivatives, organic gels, fibres, zeolites and mesoporous inorganic materials (MPS).<sup>26–30</sup> Among these supports, MPSs have attracted particular interest because of certain features such as highly specific surface area, specific pore volume and high thermal stability. However, reduction of catalytic activity of enzymes by adsorption on the MPS surface and leakage of the enzyme molecules from the mesopores are persisting problems for industrial applications.

Laccase (benzenediol:oxygen oxidoreductase, EC 1.10.3.2) is a multi-copper-bearing lignolytic enzyme, which catalyses the one-electron oxidation of many phenolic compounds with concomitant reduction of oxygen to water. Laccase is widely distributed in higher plants, some insects, few bacteria and fungi.<sup>31–33</sup> The ability of laccase to oxidize pollutants with slightly low substrate specificity has attracted interest in the use of laccase for possible use in wastewater treatment and bioremediation. In addition, laccase has a high catalytic activity, and with 2,2'-azinobis-(3-ethylbenzothiazoline-6-sulfonate)-diammonium salt (ABTS) as its electron donor, laccase can be efficiently coupled to carbon electrodes.<sup>34–37</sup> One approach towards the design of an implantable, membrane-less and bio-compatible biofuel cell comprises catalysing the oxidation of glucose at the anode using either glucose oxidase or glucose dehydrogenase enzymes, coupled to the reduction of dioxygen at the cathode by a dioxygen-reducing enzyme such as laccase. However, various laccase immobilisation methods on different solid supports have not been able to successfully

immobilise the enzyme with retention of its full catalytic activity.

Myoglobin (Mb) is an oxygen-transport protein in mammalian muscle. Mb has a molecular weight ( $M_w$ ) of about 17000 and contains a single electro-active iron heme as a prosthetic group.<sup>38,39</sup> The Fe(III)/Fe(II) redox couple of the heme protein Mb yielded standard electron-transfer rate constants about 1000-fold larger on pyrolytic graphite electrodes than free Mb in solution.<sup>40</sup> It is essential to develop adsorption and immobilization procedures and carrier materials for further bioanalytical utilization.

In this study, we investigated the encapsulation of oxidative enzyme, laccase, in ASNT hydrogel. We focused on two different aspects, namely, the length of nanotubes used, which will maintain enzyme activity and the conformation change of the enzyme in the hydrogel. With the protein immobilized in the ASNT hydrogel, the confinement effect tends to stabilize the protein molecules. First, we synthesized an ASNT hydrogel with various nanotube lengths (1, 2, 4 and 7 days ageing) to understand the effect on enzyme encapsulation and catalytic activity. Second, the conformational change of laccase was discussed. For this, the enzyme was encapsulated in ASNT hydrogel, and changes to its tertiary structure were estimated by fluorometric techniques. In addition, transparent films from the laccase-ASNT hydrogel were easily produced by a drop-coating method, and these enzyme films worked well.

The purpose of this work was to investigate the use of the oxidative enzymes, laccase and myoglobin, encapsulated in ASNT hydrogel as a new technology for stable biocatalysis. Our investigation revealed superior catalytic activity in the optimized enzyme-ASNT hydrogel composite and excellent reusability associated with structural stability.

## Experimental

### Materials

Aluminium chloride ( $\text{AlCl}_3 \cdot 6\text{H}_2\text{O}$ ) was purchased from Kanto Chemical Co., Tokyo, Japan. Sodium silicate ( $\text{Na}_4\text{SiO}_4 \cdot n\text{H}_2\text{O} : \text{SiO}_2 = 20.3 \text{ wt\%}, \text{Na}_2\text{O} = 40.1 \text{ wt\%}$ ) was purchased from Kishida Chemical Co., Osaka, Japan. Laccase (from *Trametes versicolor*, Cat. NO. 51639;  $M_w = 70 \text{ kDa}$ ;  $\text{pI} = 3.5$ ) and Mb (from equine skeletal muscle, Cat. NO. M0630;  $M_w = 17.6 \text{ kDa}$ ;  $\text{pI} = 7.3$ ) were obtained from Sigma–Aldrich, St. Louis, MO, USA. ABTS was acquired from Tokyo Chemical Industry Co., Tokyo, Japan. Fluorescein labelling Kit-NH<sub>2</sub> was obtained from Dojindo Molecular Technologies, Kumanoto, Japan. Protein assay dye reagent was purchased from Bio-Rad Laboratories, Hercules, CA, USA. All materials were of analytical grade and used as received without further purification.

### Preparation of aluminium silicate nanotube

ASNT, i.e. imogolite, was prepared according to the procedure described in a previous report (Fig. 1).<sup>24,25</sup> Sodium silicate (18.47 g,  $\text{Na}_4\text{SiO}_4$ ) and aluminium chloride (9.20 g,  $\text{AlCl}_3 \cdot 6\text{H}_2\text{O}$ ) were dissolved in 500 g of distilled water, respectively. After mixing, the solution was titrated with 1 M

sodium hydroxide (NaOH) up to pH 6.8. The resulting samples were collected by centrifugation, and the obtained precipitates were washed three times with distilled water. Adding 12 L of distilled water that was acidified with 5 M hydrochloric acid dispersed the precursor ASNT. The precursor solution was aged at 95 °C for 1, 2, 4 and 7 days, which controlled the length of ASNTs. Finally, aqueous solutions of 0.087 wt% of dispersed ASNTs were produced.

### Laccase encapsulation in ASNT hydrogel

Each heated ASNT dispersed solution (3.0 g) was adjusted to pH 7.0 with 0.4 M NaOH. Laccase solution (100  $\mu$ L, 0.5 mg mL<sup>-1</sup>) was added to the solution, and the mixture was stirred for 10 min and then kept standing for 1 h at 4 °C. The produced laccase-encapsulated ASNT hydrogel was collected by centrifugation at 6,000 rpm for 15 min. The amount of ASNT hydrogel obtained was ~100 mg.

### Characterization of laccase-ASNT hydrogel composite

The morphology of the products was characterized using a field-emission scanning electron microscope (FESEM, Hitachi S-4700, Hitachi, Tokyo, Japan). Transmission electron microscopy (TEM) images were acquired using a JEOL JEM 2010 (JOEL, Tokyo, Japan) operating at 200 kV. Fourier transform infrared spectroscopy (FT-IR) spectra were obtained using an MFT-2000, JASCO, Tokyo, Japan. For FT-IR analyses, the samples were pelletized with KBr (sample/KBr = 1:100) using a hydraulic press. Thermogravimetry and differential thermal analysis (TG and DTA) were performed on an SSC-5200, SEIKO Instrument, Tokyo, Japan. Peaks were collected from room temperature to 1050 °C (heating rate = 10 °C min<sup>-1</sup>). Atomic force microscope (AFM, scanning probe microscope, SPA-400, SII Nano Technology Inc., Tokyo, Japan) was also used to investigate the morphological characteristics of ASNT. An area of 5  $\mu$ m  $\times$  5  $\mu$ m was scanned using a 110  $\mu$ m scanner and an SI-DF20 cantilever (SII Nano Technology Inc.). Rheological properties of the ASNT hydrogel were measured using a rheometer (MCR101, Anton Paar Japan, Tokyo, Japan). A 500  $\mu$ L sample of the ASNT hydrogel was placed on a stainless parallel plate of 25 mm in

diameter, and the geometric gap was set to 1 mm. The storage modulus ( $G'$ ) and loss modulus ( $G''$ ) were measured at various strain amplitudes at  $f = 1$  Hz. In addition, the frequency dependence of both moduli of the samples was measured from 0.1 to 10.0 Hz at 25 °C. Powder X-ray diffraction (XRD) analysis was performed using a RINT2000/PC (Rigaku Co., Tokyo, Japan) model equipped with a CuK $\alpha$  source. The  $2\theta$  scanning range was set between 3° and 60°; generator settings were 40 kV and 30 mA.

### Catalytic activity of laccase encapsulated in ASNT hydrogel

The potential for applying the ASNT hydrogel as biocatalyst and biosensor based on catalytic activity was investigated using laccase. The peroxidase activity of laccase was measured using ABTS and O<sub>2</sub>. ABTS is water soluble and has a strong absorption band at 340 nm,<sup>31</sup> while its oxidized derivative is blue-green in colour and its absorption band is shifted to 420 nm. First, laccase (0.05 mg) encapsulated in ASNT hydrogel prepared in Section 2.3 (~100 mg) was added to a 100  $\mu$ L solution of ABTS and 800  $\mu$ L of a 10 mM phosphate buffer solution (pH 7.0), and then laccase in ASNT hydrogel was allowed to react for 10 min at 30 °C. Subsequently, the absorbance at 420 nm for each reaction mixture was measured using a UV-vis spectrophotometer (V-560, Jasco Co., Tokyo, Japan). In addition, an ASNT hydrogel reaction mixture without laccase was prepared as a blank, and its absorbance was measured at 420 nm. The activity of free laccase was expressed as 100%. The recyclability of laccase in hydrogel was also determined using a similar procedure.

Oxidative activity of Mb was measured by a procedure similar to that for laccase. Free Mb (0.05 mg) or Mb in ASNT hydrogel was added to a solution of 100  $\mu$ L of ABTS, 20  $\mu$ L of a 8.8 mM hydrogen peroxide solution (H<sub>2</sub>O<sub>2</sub> as an oxidant) and 780  $\mu$ L of a 10 mM phosphate buffer solution (pH 7.0), and the subsequent procedure was the same as that in the case of the laccase reaction.

No oxidative reaction occurred when using ASNT hydrogel (without laccase) under the above-mentioned reaction conditions. Each reported value is the mean of the results obtained for at least three experiments.

### Conformational changes of laccase in ASNT hydrogel

The experiments comprised monitoring the fluorescence of tryptophan residues, which gives information on the tertiary state of the protein. For analysis, laccase in hydrogel (~100 mg) was suspended in 3 mL of a 10 mM phosphate buffer solution (pH 7.0). After stirring in the dark at 25 °C for 30 min, fluorescence emission spectra of laccase were recorded at excitation and fluorescence wavelengths of 280 nm and from 300 to 450 nm, respectively.

### Drop-coating of Laccase-ASNT hydrogel composites

Laccase was conjugated with fluorescein isothiocyanate (FITC) according to the procedure provided from supplier (Dojindo Molecular Technologies). FITC-conjugate laccase (100  $\mu$ L; 1 mg 100  $\mu$ L<sup>-1</sup>) was mixed in 3 mL of 1-day ASNT solution

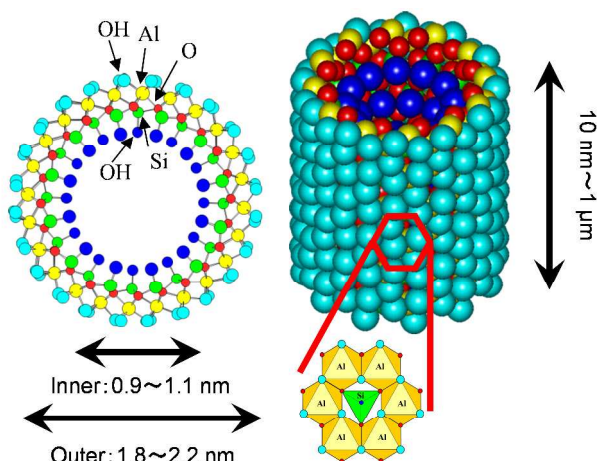


Fig. 1 Structural illustration of the ASNT, imogolite, synthesized in this study.

adjusted to pH 7.0, and the mixture was stirred at 4 °C for 10 min. The resulting solution (150  $\mu$ L) was drop-coated on 15 mm-diameter cover glass cover slip (cleaned by acetone), and the film was dried at room temperature for 24 h. In addition, the dot coating of laccase in 1-day ASNT solution was performed using 1  $\mu$ L of the above solution on the cover slip. The obtained samples were immediately observed using a fluorescent microscope (BX51, Olympus Co., Tokyo, Japan) with a band-pass filter.

## Results and discussion

### Encapsulation of laccase in ASNT hydrogels and their characterization

With this AFM specimen preparation method, direct observation of individual ASNT with definite dimensions could be achieved. It also makes the investigation of the growth process of the nanotubes possible because the concentration and the exact length of the nanotubes can be quantitatively analysed through our controlled experiments. Figure 2 shows AFM images of the ASNT obtained after heating periods of 1, 2, 4 and 7 days. As shown in Fig. 2, a small number of the nanotubes with diameters of 2–3 nm could be discerned out of the amorphous product, indicating the formation of ASNT as early as after a one day reaction. The lengths of the nanotubes are below  $\sim$ 50 nm. For the rest of the images in Fig. 2, the concentration of the ASNT increases with reaction time, especially after two days, and the length of the nanotubes falls into a fairly large range. The lengths of ASNTs were increased when the reaction periods were longer, and over 1  $\mu$ m and 3  $\mu$ m of ASNTs were obtained after a heating period of 4 days and 7 days, respectively. Moreover, it should be noted that the diameter of the nanotubes remains almost unchanged throughout the synthesis.

The morphology of the freeze-dried ASNT samples was

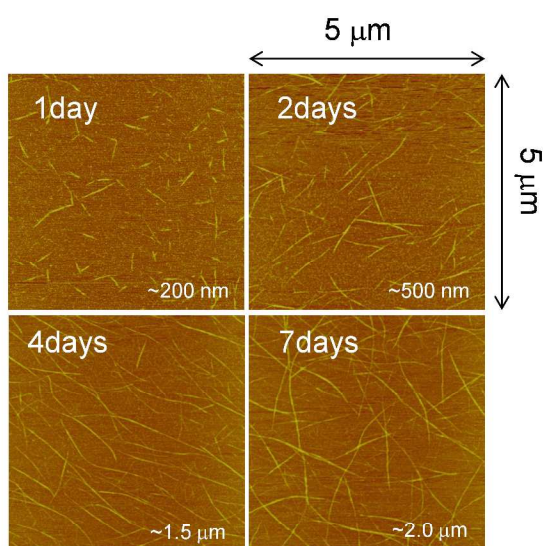


Fig. 2 AFM images of ASNT heated for each heating period (1, 2, 4 and 7 days).

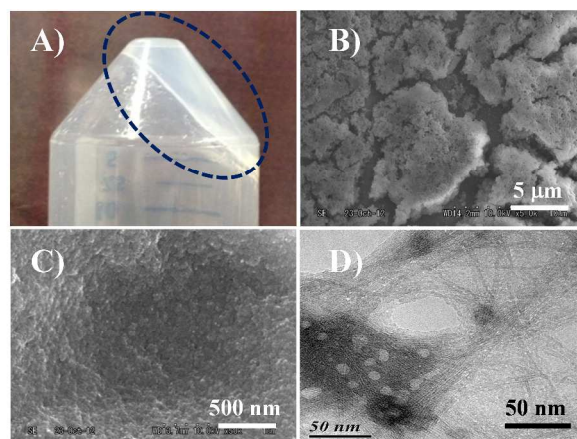


Fig. 3 FE-SEM and TEM images of ASNT hydrogel heated for 1 day. (A) ASNT hydrogel prepared from the same solution, SEM images at (B) low-magnification, (C) high-magnification and (D) TEM, samples was prepared directly by dilution of ASNT dispersion solutions.

characterized using FE-SEM and transmission electron microscopy (TEM). Figure 3A shows the bare ASNT hydrogel prepared according to procedure provided in the experimental section. Once the surrounding pH was brought up to pH 7.0 using 0.4 M NaOH, turbid and non-flowing hydrogel was formed after centrifugation of the mixture. The weight of ASNT hydrogel obtained was 108 mg, prepared from the 3 g of 1-day ASNT dispersed solution, and 1.6 mg of freeze-dried solid material was obtained from the ASNT hydrogel. This result indicated that 1.5% (w/w) (98.5% water) ASNT was present in the hydrogel. Subsequently, the mixture was manually mixed for 30 s, and thus the turbidity disappeared within 15–20 s and the mixture turned into a translucent solution. Figures 3B (low-magnification) and 3C (high-magnification) shows FE-SEM images of ASNT hydrogel. The large aggregates with 1–10  $\mu$ m size were formed from the small particles (<50 nm) of ASNT bundles. Figure 3D shows ASNT bundles forming a continuous network structure, having lengths between 100 and 300 nm and widths between 30 and 40 nm. Bundles of  $\sim$ 10–20 nanotubes were observed in the ASNT dispersion solution.

Figure 4A shows the XRD patterns of the bare ASNT and laccase-ASNT composites. In this study, the ASNTs prepared showed typical peaks at 26° and 40° that correspond to amorphous ASNT, and a broad peak at  $\sim$ 9° shows that tubular units of ANSTs exist. The XRD patterns after encapsulation of laccase within ASNT hydrogel was unchanged compared to bare ASNT hydrogel, indicating that enzyme encapsulation have no effect on the structure of ASNTs.

TG-DTA curves for bare ASNT and laccase-ASNT composites are shown in Fig. 4B. The  $\sim$ 15% weight loss observed for both composites are observed from 100 to 120 °C due to the presence of moisture (H<sub>2</sub>O). The weight loss for samples between 350 and 450 °C is assigned to the decomposition of the enzyme's protein component, as shown in



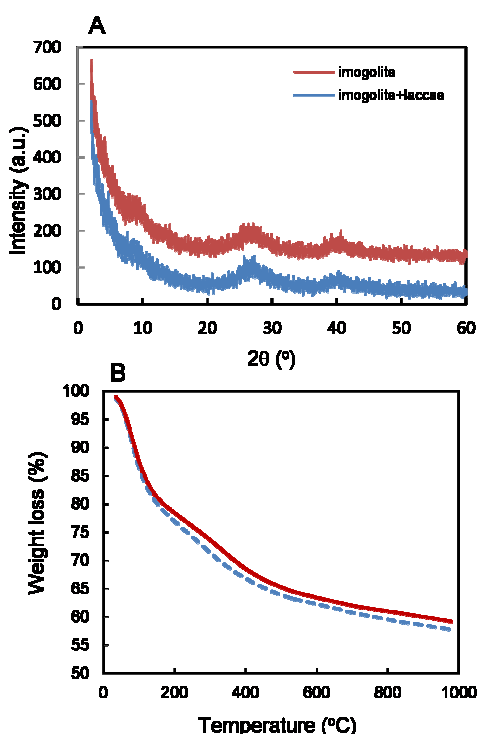


Fig. 4 (A) XRD patterns and (B) TG-DTA curves of 1-day ASNT hydrogel and laccase encapsulated ASNT hydrogel. Red line, bare ASNT hydrogel; blue line, laccase-ASNT hydrogel composite.

Fig. 4B. The weight loss percentage of the laccase-ASNT composite is 2%–3%, which agrees with the value corresponding to the weight of the enzyme inside the silica (0.05 mg enzyme/~1.50 mg total mass of ASNT freeze-dried gel).

ASNT gel encapsulation of laccase was also monitored by

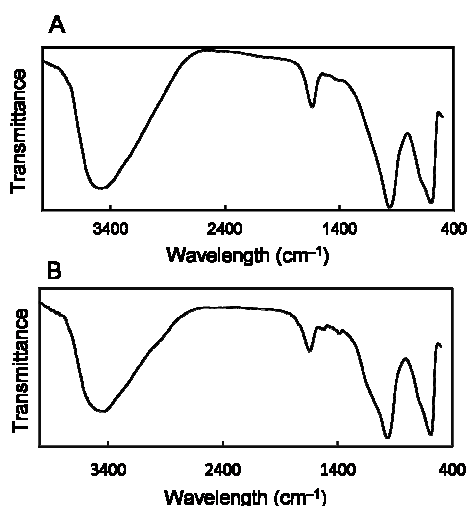


Fig. 5 FT-IR spectra of (A) 1-day ASNT hydrogel and (B) laccase encapsulated 1-day ASNT hydrogel.

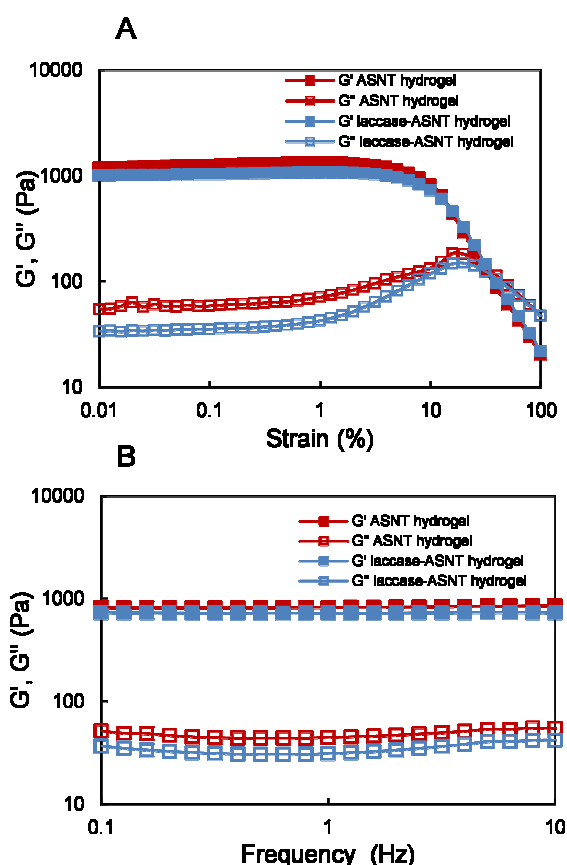


Fig. 6 (A) Strain sweep measurement and (B) Frequency sweep measurement on 1-day ASNT hydrogel and laccase-encapsulated ASNT hydrogel. Red line, bare ASNT hydrogel; blue line, laccase-ASNT hydrogel composite.

FT-IR spectroscopy (Fig. 5A). The characteristic peaks of bare ASNT were observed at 960 cm<sup>-1</sup>, corresponding to the stretching of Al–O–Si group, and a peak at 1060 cm<sup>-1</sup> could be attributed to silica vibrations (Si–O–Si). The absorption bands observed at 3000–3600 cm<sup>-1</sup> could be assigned to the OH vibrational modes of hydroxyl groups. The H–O–H bending of water is observed at 1640 cm<sup>-1</sup>. The FT-IR spectrum shown in Fig. 5B indicated a N–H deformation vibration band at 1530 cm<sup>-1</sup> amides, and showed peaks for C–H stretching from 2830 to 2960 cm<sup>-1</sup>, corresponding to the CH<sub>2</sub> of proteins, suggesting the encapsulation of laccase in the ASNT gel.

The linear viscoelasticity range was observed until  $\gamma < \sim 8\%$  and the crossover of G' and G'' occurred at  $\gamma = 30\%–40\%$  on bare and laccase-encapsulated ASNT hydrogel samples (Fig. 6A). The shear stress applied at the deformation points of both samples were measured as  $\sim 60$  Pa. The onset of non-linearity could be interpreted as the onset of gel network breaking. The following frequency sweep test was conducted under an applied strain of 1%, where the samples are confirmed to be in the linear viscoelasticity range. The viscoelastic strength of the ASNT hydrogel indicated closed to 1,000 Pa of G' for 1-day ASNT and small difference was observed for the hydrogel after

encapsulation of enzymes (Fig. 6B).  $G'$  and  $G''$  moduli showed plateau regions, and  $G' > G''$  for both samples throughout the frequency, suggesting that the samples behaved as a solid structure. The laccase encapsulated ASNT sample had a  $G'$  of  $\sim 700$  Pa, which was close to the value obtained for bare ASNT hydrogel,  $\sim 800$  Pa. A gel with this stiffness is expected to be injectable using a syringe and needle, because one report showed that a peptide gel with a storage modulus of  $\sim 480$  Pa was injectable.<sup>41</sup> The gel forming ability of the ASNT and its properties (strength) were hardly affected by the enzyme encapsulation; thus, this ASNT hydrogel achieved sufficient viscoelastic strength and is applicable as a carrier material for an enzyme or other biomolecules for applications such as drug delivery or biocatalysis.

### Oxidative activity of laccase in ASNT hydrogels

Figure 7A shows the oxidation activity of laccase encapsulated in the ASNT hydrogel. The activity of free laccase in solution was used as control and was considered to be 100%. Maximum oxidation activity was observed for laccase encapsulated in the 1-day ASNT hydrogel; notably, this activity (134% relative activity) was higher than free laccase in solution. The oxidation activity of laccase-ASNT hydrogel decreased when heating time in ASNT preparation was increased and was 97% for 2 days, 78% for 4 days and 61% for 7 days, respectively.

Furthermore, we explored the cycle performance of laccase encapsulated in ASNT hydrogel, as shown in Fig. 7B. During the test, the remaining activity was recorded after each cycle. The laccase-ASNT hydrogel retained  $\sim 100\%$  of its initial

Table 1 Kinetic parameters of laccase encapsulated in ASNT hydrogels prepared from the solution aged for each period

ASNT-laccase	$K_m$ (mM)	$V_{max}$ ( $\mu\text{mol min}^{-1}\text{mg}^{-1}$ )
1day	1.39	1.00
2days	1.77	1.23
4days	1.79	0.93
7days	1.91	1.03
Free	2.85	1.59

activity, even after nine repetitions. This proves the recyclability of laccase encapsulated in ASNT hydrogel. This could be attributed to the decreased enzyme release in ASNT hydrogel because of the strong interaction between the enzyme and ASNT networks.

### Enzyme kinetics and conformational changes of laccase encapsulated in ASNT hydrogel

To evaluate the difference in oxidation activity of laccase-encapsulated ASNT hydrogel, the kinetic properties of the composite prepared from ASNTs of different nanotube sizes, including the Michealis constant,  $K_m$ , and the maximum rate,  $V_{max}$ , were determined for the enzyme reactions (Table 1). The  $K_m$  values, which are given by the concentration of substrate that leads to half-maximal velocity, for all hydrogels were smaller than that of the free laccase ( $K_m = 2.85$  mM). These results show that ASNT hydrogels can facilitate substrate diffusion within their matrices. Particularly, the  $K_m$  value of laccase encapsulated in the 1 day ASNT hydrogel ( $K_m = 1.39$  mM) was notably higher when compared with that of the other samples (1.77 mM for 2 days, 1.79 mM for 4 days and 1.91 mM for 7 days), and hence achieved enhanced apparent enzymatic activity.  $V_{max}$  values, the maximum velocity or rate at which the enzyme catalysed a reaction, of laccase-ASNT hydrogel composites was slightly lower compared to that of the free laccase.

Furthermore, we analysed the changes in the tertiary structure of laccase by tryptophan fluorescence spectra to study the influence of the interactions between the enzyme and ASNT hydrogel. Fluorescence from the amino acid tryptophan has long been known to be sensitive to the polarity of its local environments. It is well understood that the spectral parameters of tryptophan fluorescence emission are sensitive to the environment of tryptophans and that a protein's tryptophans can give insights on environmental changes during events such as folding or unfolding.<sup>42</sup> For example, the  $\lambda_{max}$  of many proteins' emission scans will red-shift upon unfolding as the tryptophans become more exposed to polar solvents. From the amino acid sequence of *Trametes versicolor* laccase obtained from a protein data bank (ID: 1GTC), this enzyme has seven tryptophans inside its structure, and relatively hydrophobic amino acids (valine, leucine, etc) exist on its surface (Fig. 8A). Figure 8B shows the fluorescence emission spectra of

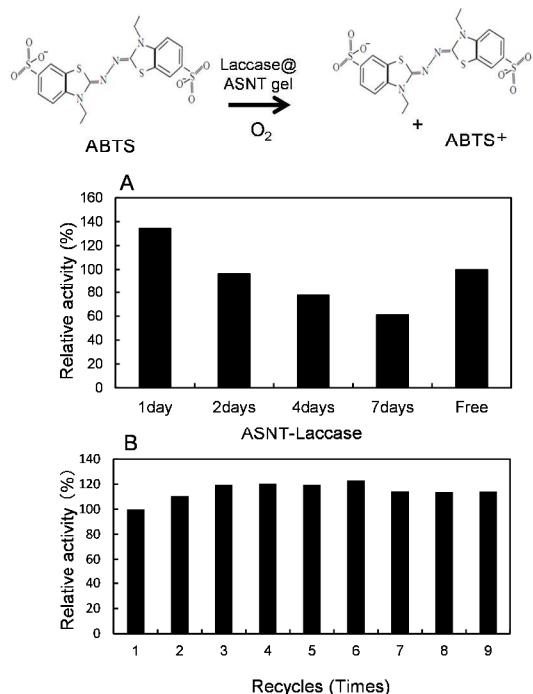


Fig. 7 (A) Catalytic activity of laccase encapsulated in ASNT hydrogel prepared from the solution aged for each period. (B) Recyclability of enzyme in 1-day ASNT hydrogel.

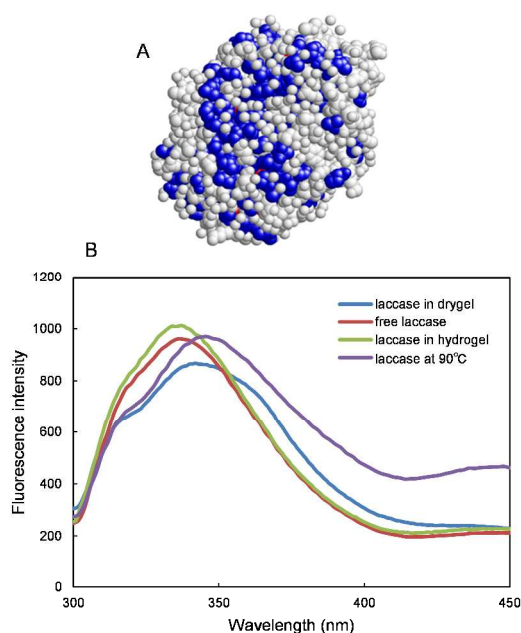


Fig. 8 (A) Three-dimensional structure of laccase, obtained from Protein Data Bank; ID: 1GYC. Red balls for tryptophans; blue balls for hydrophobic amino acids. (B) Conformational changes of laccase encapsulated in 1-day ASNT hydrogel, determined by tryptophan fluorescence spectra.

tryptophan residues. As evidenced from the spectra, the conformational changes of the protein were observed after thermal treatment for 30 min at 90 °C, i.e.  $\lambda_{\text{max}}$  was shifted from 338 (free laccase) to 346 nm. In addition, free laccase after thermal treatment, as described above, has no oxidation activity, indicated by an 8 nm red-shift in  $\lambda_{\text{max}}$ . Laccase in dry gel prepared by freeze-drying of ASNT hydrogel has extremely low (<10%) relative activity compared with free laccase. In this case,  $\lambda_{\text{max}}$  of the laccase was red-shifted to 344 nm. However, laccase encapsulated in ASNT hydrogel generated similar tryptophan fluorescence spectral profiles to those of free laccase in solution with equivalent  $\lambda_{\text{max}}$  and emission intensity. From these results, no conformational changes to laccase were observed in ASNT hydrogel and its high oxidation activity was retained inside the hydrogel matrix.

#### Coating of the laccase-ASNT hydrogel on glass and its activity

Since laccase is a dioxygen-reducing enzyme, it could be used for the cathode of a bio-fuel. For laccase-ASNT hydrogel to be used in various applications such as biofuel cell, biosensor and bioremediation, the hydrogel was coated on glass cover slips. The suspension (150  $\mu\text{L}$ ) was prepared by mixing FITC-labelled laccase and an ASNT dispersion solution, which was then dropped on a glass cover slip, and the resulting ASNT film was dried at room temperature for 24 h. The resulting transparent film was easily prepared and the laccase adsorbed on the nanotubes was found to be uniformly coated on the glass

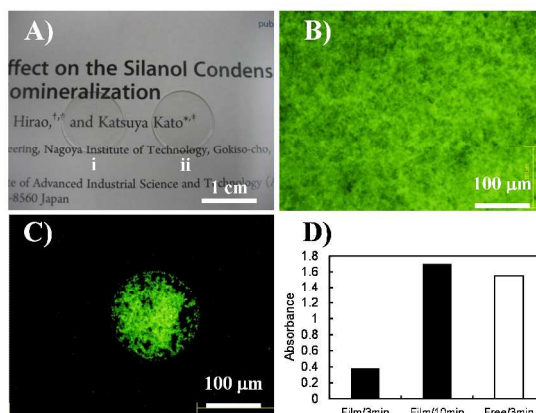


Fig. 9 Drop-coating of laccase in 1-day ASNT hydrogel on cover glass slip. (A) Image of laccase-ASNT on glass slip (15 mm  $\phi$ ). (i) laccase-ASNT film and (ii) no hydrogel on glass slip. (B) fluorescence microscopy of FITC-laccase in ASNT hydrogel coated on a slide. (C) fluorescence microscopy of FITC-laccase in ASNT hydrogel by dot-coating. (D) catalytic activity of laccase in ASNT hydrogel coated on a slide.

from fluorescence microscopy images (Figs. 9A and 9B). In addition, 1  $\mu\text{L}$  of the above suspension was dot coated on the same glass cover slip. An approximately 100  $\mu\text{m}$  diameter-sized dot of laccase-ASNT composite was obtained and the laccase was well distributed within the dot printed area (Fig. 9C). The enzyme activity of laccase-ASNT films were verified by ABTS oxidation with a similar procedure to the one used to test the laccase-ASNT hydrogel. Its activity (0.38 abs, as determined by absorbance of oxidized ABTS at 420 nm) was lower, about 25%, than that measured for free laccase (1.55 abs), indicating that the conformation of laccase was changed during preparation of the film, as was the case after the freeze-drying process described above. However, as enzyme reaction time was increased, activity rate was improved (1.70 abs), meaning that these laccase films are still active and are reusable (Fig. 9D). These results are very attractive for further bio-applications.

#### Myoglobin encapsulation in ASNT hydrogels

The oxidative catalytic activity of free Mb (0.05 mg) was also evaluated under the same reaction conditions. The enzyme reaction was performed with ABTS and  $\text{H}_2\text{O}_2$  as an oxidant. No reaction occurred in the absence of Mb (on ASNT hydrogel) under these conditions. Figure 10A reveals that Mb's activity was markedly reduced (by ~30% relative activity) compared to free laccase. In addition, cycle testing of myoglobin encapsulated in ASNT hydrogel was performed, and remaining activities were recorded after each cycle. Mb encapsulated in ASNT hydrogel retained ~80 % of its initial activity even after five repeated reactions. These results indicate that encapsulated Mb experienced little leaching from the hydrogel.



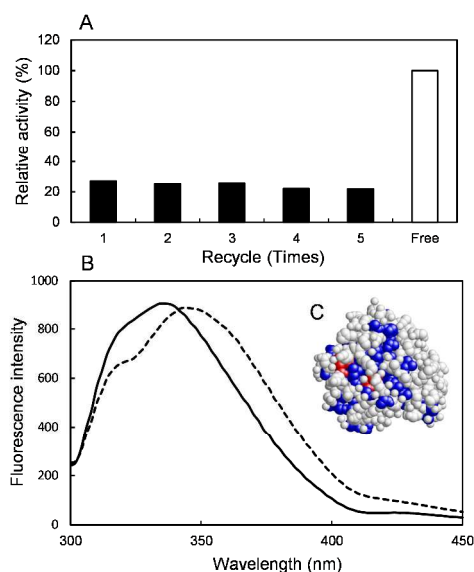


Fig. 10. (A) Catalytic activity of Mb encapsulated in 1-day ASNT hydrogel. (B) Conformational changes of Mb encapsulated in 1-day ASNT hydrogel, determined by tryptophan fluorescence spectra: solid line, free Mb solution; dotted line, Mb encapsulated in ASNT hydrogel. (C) Three-dimensional structure of Mb, obtained from Protein Data Bank; ID: 1NPF. Red balls for tryptophans; blue balls for hydrophobic amino acids.

Figure 10B shows the fluorescence emission spectra of tryptophan residues from free and encapsulated Mb. Mb from horse heart contains two tryptophans in its entire amino acid sequence (protein data bank; ID: 1NPF, Fig. 10C). The highest emission intensities are 334 nm and 344 nm for free Mb and Mb encapsulated in ASNT hydrogel, respectively. The maximum peak,  $\lambda_{\text{max}}$ , was red-shifted by 10 nm, suggesting partial unfolding of the tertiary structure or greater exposure of tryptophan residues to the solvent. The reduction of Mb activity in the ASNT hydrogel, unlike laccase, was due to a conformational change of the protein within the ASNT hydrogel.

## Conclusions

Laccase was encapsulated in ASNT hydrogel carefully prepared at pH 7, while maintaining protein activity and stability. The obtained ASNT hydrogels were fully characterized by FE-SEM, TEM, XRD, TG-DTA and FT-IR. In addition, rheological properties of the hydrogel with and without laccase were also determined by strain sweep and frequency sweep measurements.  $G'$  and  $G''$  moduli showed plateau regions, and  $G' > G''$  for both samples throughout the frequency range, suggesting that the samples behaved as solid structures. Encapsulation of laccase did not affect the gel properties of the ASNT hydrogel. The performance of the laccase-ASNT hydrogel was evaluated on the basis of their enzyme activity and cycling characteristics to determine the

optimal structure and length of the nanotube for enzyme encapsulation. Laccase encapsulated in ASNT hydrogel prepared from nanotube suspension heated for 1 day (1-day ASNT hydrogel), which has the shortest length of nanotubes tested, exhibited a higher activity than those of other ASNT hydrogels. Moreover, the rate of activity of laccase-ASNT hydrogel composites was 40% higher than that of free laccase activity because of an increase in substrate affinity and high conformational stability produced by the hydrogel networks. Furthermore, biocatalysts comprising laccase encapsulated in an ASNT hydrogel remained stable through repeated reaction cycles.

Finally, the laccase-ASNT hydrogel composite was easily prepared in film morphology by a drop-coating method, and the obtained enzyme films worked well on the glass cover slip. Therefore, this laccase-ASNT hydrogel system is a promising candidate for applications such as bio sensors, biofuel cells and biocatalysts.

## Acknowledgements

We thank Mr. Norito Morishita of the Aichi Institute of Technology for his technical assistance.

## Notes and references

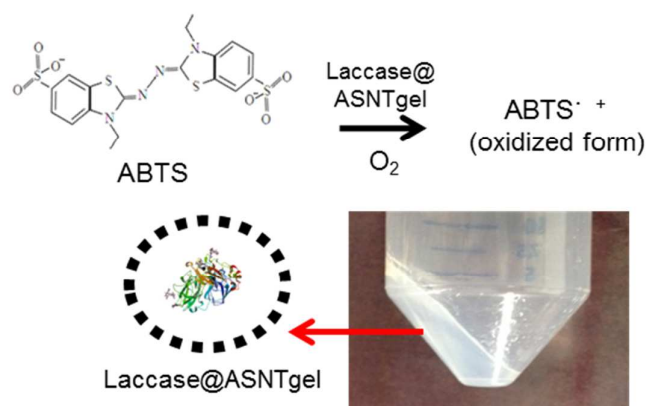
<sup>a</sup> National Institute of Advanced Industrial Science and Technology (AIST), 2266-98 Anagahora, Shimoshidami, Moriyama-ku, Nagoya 463-8560, Japan. E-mail: katsuya-kato@aist.go.jp; Fax: +81 52 736 7405; Tel: +81 52 736 7551

<sup>b</sup> Department of Frontier Materials, Nagoya Institute of Technology, Gokiso-cho, Showa-ku, Nagoya, Aichi 466-8555, Japan.

- 1 G. Orive, R.M. Hernández, A.R. Gascón, R. Calafiore, T.M.S. Chang, P. De Vos, G. Hortelano, D. Hunkeler, I. Lacík, A.M.J. Shapiro and J. L. Pedraz, *Nature Medicine*, 2003, **9**, 104.
- 2 Z. Fang, B. Bhandaria, *Trends in Food Sci. Technol.*, 2010, **21**, 510.
- 3 P.B. Salunkhe, P.S. Shembekar, *Sustain. Energy. Rev.*, 2012, **16**, 5603.
- 4 I.G. Loscertales, A. Barrero, I. Guerrero, R. Cortijo, M. Marquez, A.M. Gañán-Calvo, *Science*, 2002, **295**, 1695.
- 5 F. Hof, S.L. Craig, C. Nuckolls, J. Rebek, Jr., *Angew. Chem. Inter. Edn.*, 2002, **41**, 1488.
- 6 G. Lu, S. Li, Z. Guo, O.K. Farha, B.G. Hauser, X. Qi, Y. Wang, X. Wang, S. Han, X. Liu, J.S. DuChene, H. Zhang, Q. Zhang, X. Chen, J. Ma, S.J. Loo, W.D. Wei, Y. Yang, J.T. Hupp, F. Huo, *Nature Chem.*, 2012, **4**, 310.
- 7 B.C. Dave, B. Dunn, J.S. Valentine, J.I. Zink, *Anal. Chem.*, 1994, **66**, 1120A.
- 8 A.C. Pierre, *Biocatal. Biotrans.*, 2004, **22**, 145.
- 9 D. Arcos, M. Vallet-Regí, *Acta Biomaterialia*, 2010, **6**, 2874.
- 10 K. Kato, M. Nishida, K. Ito, M. Tomita, *Appl. Surf. Sci.*, 2012, **262**, 69.
- 11 P.D.G. Cradwick, V.C. Farmer, J.D. Russell, C.R. Masson, K. Wada, N. Yoshinaga, *Nature Phys. Sci.*, 1972, **240**, 187.
- 12 K. Tamura, K. Kawamura, *J. Phys. Chem. B*, 2002, **106**, 271.
- 13 H. Yang, C. Wang, Z. Su, *Chem. Mater.*, 2008, **20**, 4484.
- 14 K. Yamamoto, H. Otsuka, A. Takahara, *Polymer J.*, 2007, **39**, 1.

- 15 L. Guimarães, A.N. Enyashin, J. Frenzel, T. Heine, H.A. Duarte, G. Seifert, *ACS Nano*, 2007, **1**, 362.
- 16 X. Qia, H. Yoona, S. Lee, J. Yoon, S. Kim, *J. Ind. Eng. Chem.*, 2008, **14**, 136.
- 17 Y. Kuroda, M. Tamakoshi, J. Murakami, K. Kuroda, *J. Ceram. Soc. Jpn.*, 2007, **115**, 233.
- 18 Z. Hu, X. Lu, J. Gao, *Adv. Mater.*, 2001, **13**, 1708.
- 19 A.S. Hoffman, *Adv. Drug Delivery Rev.*, 2012, **64**, 18.
- 20 D.J. Beebe, J.S. Moore, J.M. Bauer, Q. Yu, R.H. Liu, C. Devadoss, B. Jo, *Nature*, 2000, **404**, 588.
- 21 N. Inoue, H. Otsuka, S.-I. Wada, A. Takahara, *Chem. Lett.*, 2006, **35**, 194.
- 22 N. Jiravanichanun, K. Yamamoto, K. Kato, J. Kim, S. Horiuchi, W. Yah, H. Otsuka, A. Takahara, *Biomacromolecules*, 2012, **13**, 276.
- 23 W. Ma, W. Yah, H. Otsuka, A. Takahara, *J. Mater. Chem.*, 2012, **22**, 11887.
- 24 D. Lee, H. Maeda, A. Obata, K. Inukai, K. Kato, T. Kasuga, *Adv. Mater. Sci. Eng.*, 2013, Article ID 169721, 6 pages.
- 25 S. Yamazaki, H. Maeda, A. Obata, K. Inukai, K. Kato, T. Kasuga, *J. Nanomater.*, 2012, Article ID 463768, 7 Pages.
- 26 C. Mateo, J.M. Palomo, G. Fernandez-Lorente, J.M. Guisan, *Enzyme Microbial Technol.*, 2007, **40**, 1451.
- 27 Z. Wang, L. Wan, Z. Liu, X. Huang, Z. Xu, *J. Mol. Catal. B: Enzym.*, 2009, **56**, 189.
- 28 A. Sassolas, L.J. Blum, B.D. Leca-Bouvier, *Biotechnol. Adv.*, 2012, **30**, 489.
- 29 Y. Masuda, S. Kugimiya, K. Murai, A. Hayashi, K. Kato, *Coll. Surf. B: Biointerfaces*, 2013, **101**, 26.
- 30 Y. Masuda, S. Kugimiya, Y. Kawachi, K. Kato, *Chem. Lett.*, 2013, **42**, 1252.
- 31 T. Saito, P. Hong, K. Kato, M. Okazaki, H. Inagaki, S. Maeda, Y. Yokogawa, *Enzyme Microbial Technol.*, 2003, **33**, 520.
- 32 A. Leonowicz, N. Cho, J. Luterek, A. Wilkolazka, M. Wojtas-Wasilewska, A. Matuszewska, M. Hofrichter, D. Wesenberg, J. Rogalski, *J. Basic Microbiol.*, 2001, **41**, 185.
- 33 K. Piontek, M. Antorini, T. Choinowski, *J. Biological Chem.*, 2002, **277**, 37663.
- 34 A.M. Mayer, R.C. Staples, *Phytochemistry*, 2002, **60**, 551.
- 35 E. Abadulla, T. Tzanov, S. Costa, K. Robra, A. Cavaco-Paulo, G.M. Gübitz, *Appl. Environ. Microbiol.*, 2000, **8**, 3357.
- 36 M. Smolander, H. Boer, M. Valkiainen, R. Roozeman, M. Bergelin, J. Eriksson, X. Zhang, A. Koivula, L. Viikari, *Enzyme Microbial Technol.*, 2008, **43**, 93.
- 37 A. Szczupak, D. Kol-Kalman, L. Alfonta, *Chem. Commun.*, 2012, **48**, 49.
- 38 A. Ostermann, R. Waschipky, F.G. Parak, G.U. Nienhaus, *Nature*, 2000, **404**, 205.
- 39 U. Flögel, M.W. Merx, A. Gödecke, U.K.M. Decking, J. Schrader, *Proc. Natl. Acad. Sci. USA*, 2001, **98**, 735.
- 40 J.F. Rusling, A.F. Nassar, *J. Am. Chem. Soc.*, 1993, **115**, 11891.
- 41 E.L. Bakota, Y. Wang, F.R. Danesh, J.D. Hartgerink, *Biomacromolecules*, 2011, **12**, 1651.
- 42 J.T. Vivian, P.R. Callis, *Biophysical J.*, 2001, **80**, 2093.

## Graphical Abstract



January 10 2014

## Cover Letter

Dear Editor-in-Chief,

*New Journal of Chemistry*

Please find enclosed our manuscript entitled “*Effective encapsulation of laccase in an aluminum silicate nanotube hydrogel*,” which we request you to consider for publication as an original article in *New Journal of Chemistry*.

Encapsulation technologies have attracted considerable attention because of an increased interest in fields such as biotechnology, medicine, pharmaceuticals, catalysis, ecology and nutrition. Encapsulation can concentrate and shield the biomolecules to protect them in a defined volume and to create a single compartment that represents a microenvironment separated from the outer environment. Biomolecules have industrial applications based on various chemical and physical methods such as solvent evaporation, coacervation, interfacial polymerization and matrix (organic or inorganic) entrapment.

Typical aluminum silicate nanotube material, imogolite, is a naturally occurring single-walled nanotubular aluminum silicate (ASNT) with an empirical formula of  $(\text{OH})_3\text{-Al}_2\text{O}_3\text{SiOH}$ . In addition, the dispersibility of ASNT in water changes dramatically depending on pH, i.e. ASNT disperses as monofilament or thin bundle in acidic water (pH 4); in contrast, ASNT assembles into thick bundles or networks with an increase in pH, and the resulting hydrogels formed around pH 7. In this study, we investigated the encapsulation of the oxidative enzyme, laccase, in an ASNT hydrogel. We focused on two different aspects, namely, the effects of nanotube length on enzyme activity and the conformational changes of enzymes in the hydrogel.

The enzyme encapsulated in ASNT hydrogel worked well; notably, laccase-ASNT hydrogel prepared from the shortest nanotubes exhibited higher activity than free laccase in solution because of an improvement in the substrate affinity of the enzyme encapsulated inside ASNT hydrogel. The cycle performance of the encapsulated enzyme indicates no enzyme is released from the ASNT hydrogel. In addition, the laccase-ASNT hydrogel was easily prepared into transparent thin films on a glass slip, and these enzyme films were still active.

To the best of our knowledge, this study is the first report of the development of highly active and stable laccase encapsulated in ASNT hydrogel. We therefore believe that the results of this study are relevant to the readers of *New Journal of Chemistry*. The manuscript has been carefully reviewed by an experienced editor whose first language is English, and who specializes in editing papers written by scientists whose native language is not English.

This manuscript has not been published or presented elsewhere, and is not under consideration by another journal. All study participants have provided informed consent and the study design was approved by the appropriate ethics review boards. All of the authors have approved the manuscript and agree with submission to your esteemed journal. There are no conflicts of interest to declare.

Thank you for your time and consideration. We look forward to hearing from you at your earliest convenience.

Sincerely,

Dr. Katsuya KATO,

E-mail: katsuya-kato@aist.go.jp; TEL: +86-52-736-7551

National Institute of Advanced Science and Technology (AIST)

2266-98 Anagahora, Shimoshidami, Moriyama, Nagoya, 463-8560, Japan